

Joint Beamforming and Power Control for Throughput Maximization in IRS-assisted MISO WPCNs

Yuan Zheng, Suzhi Bi, Ying-Jun Angela Zhang, Xiaohui Lin, and Hui Wang

Abstract—Intelligent reflecting surface (IRS) is an emerging technology to enhance the energy- and spectrum-efficiency of wireless powered communication networks (WPCNs). In this paper, we investigate an IRS-assisted multiuser multiple-input single-output (MISO) WPCN, where the single-antenna wireless devices (WDs) harvest wireless energy in the downlink (DL) and transmit their information simultaneously in the uplink (UL) to a common hybrid access point (HAP) equipped with multiple antennas. Our goal is to maximize the weighted sum rate (WSR) of all the energy-harvesting users. To make full use of the beamforming gain provided by both the HAP and the IRS, we jointly optimize the active beamforming of the HAP and the reflecting coefficients (passive beamforming) of the IRS in both DL and UL transmissions, as well as the transmit power of the WDs to mitigate the inter-user interference at the HAP. To tackle the challenging optimization problem, we first consider fixing the passive beamforming, and converting the remaining joint active beamforming and user transmit power control problem into an equivalent weighted minimum mean square error (WMMSE) problem, where we solve it using an efficient block-coordinate descent (BCD) method. Then, we fix the active beamforming and user transmit power, and optimize the passive beamforming coefficients of the IRS in both the DL and UL using a semidefinite relaxation (SDR) method. Accordingly, we apply a block-structured optimization (BSO) method to update the two sets of variables alternately. Numerical results show that the proposed joint optimization achieves significant performance gain over other representative benchmark methods and effectively improves the throughput performance in multiuser MISO WPCNs.

Index Terms—Wireless powered communication networks, intelligent reflecting surface, multiuser MISO, resource allocation.

I. INTRODUCTION

With the advent of Internet-of-Things (IoT) era, tens of billions of wireless devices (WDs) are envisioned to be interconnected, which inevitably induce the explosion of mobile data traffic and the ever-growing demands for higher data rates. The demand for dramatic network capacity increase and ubiquitous connectivity in IoT networks boosts the research on promising wireless technologies, such as millimetre wave (mmWave), ultra-dense network (UDN) and massive multiple-input multiple-output (mMIMO) technologies [1]. However, their advantageous communication performance often comes at a cost of

high network energy consumption and/or hardware expense. To address this problem, wireless powered communication networks (WPCNs) have been proposed [2]–[4] to use dedicated wireless energy transferring nodes to power the operation of communication devices. Compared with its conventional battery-powered counterpart, the WPCN has its advantages in lowering the operating cost and improving the robustness of communication service especially in low power applications, such as sensor and IoT networks. However, the major technical challenge in WPCNs lies in the low power transfer efficiency over long distance, resulting very limited harvested energy by the distributed WDs. Although several energy-efficient techniques, including user cooperation [5], ambient backscatter communication [6], multi-antenna technique [7], have been proposed to address this problem, the low energy transfer efficiency induced by the wireless channel attenuation is still a fundamental performance bottleneck of WPCN systems.

Recently, intelligent reflecting surface (IRS) technology has received widespread attentions of its application in wireless communications [8]. In particular, an IRS comprises a massive number of reconfigurable reflecting elements and a smart controller. Each element reflects impinging electromagnetic waves with a controllable amplitude variation and phase shift using the IRS controller. By properly adjusting the reflecting elements of IRS, the reflected signals are coherently combined with those from the other paths at the receiver to maximize the signal strength. Compared to the use of conventional amplify-and-forward (AF) or decode-and-forward (DF) relay, IRS merely changes the end-to-end channel through passive reflection without amplifying or re-encoding the received signals. The recent advance in meta-surface technology [9] makes it feasible to reconfigure the reflecting coefficients in real time, thus greatly enhancing the applicability of IRS under wireless fading channel. The integration of IRS technique in wireless communication network leads to many new technological innovations and networking paradigms. In terms of the circuit implementations, practical IRS circuits include conventional reflect-arrays [10], liquid crystal surfaces [11], and software-defined meta-materials [12], among others. For new networking schemes, the utilization of IRS was extended to various communication scenarios, such as backscatter communication system [13], cognitive radio network [14], and the UAV-based communication scenario [15].

The essential advantage of deploying IRS lies in its ability to alter the wireless propagation environment to enhance the end-to-end channel strength in a passive and energy-efficient manner.

Y. Zheng, S. Bi, X. Lin, and H. Wang are with the College of Electronics and Information Engineering, Shenzhen University, Shenzhen, China, 518060 (email: zhyu@szu.edu.cn; xhlin@szu.edu.cn; wanghsz@szu.edu.cn). S. Bi is also with the Peng Cheng Laboratory, Shenzhen, China, 518066.

Y. J. Zhang is with the Department of Information Engineering, The Chinese University of Hong Kong, Hong Kong (email: yjzhang@ie.cuhk.edu.hk).

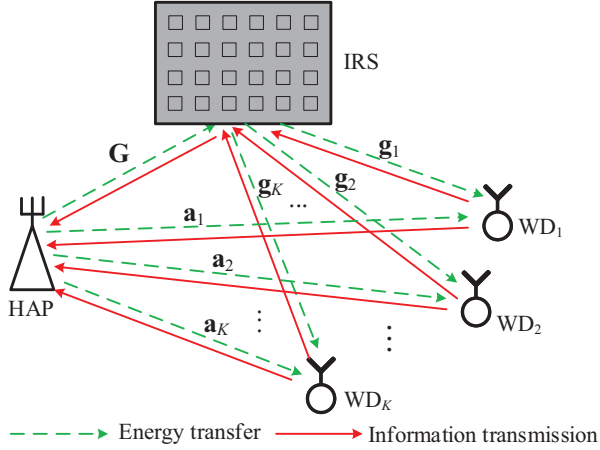


Fig. 1. The network structure of our proposed IRS-aided MISO WPCN.

This makes IRS a promising solution to tackle the fundamental performance constraints of WPCN. A large body of research on IRS-assisted WPCN has recently emerged in the literature [16]–[22]. For instance, the authors in [16] considered a joint design of active beamforming at the base station (BS) and passive beamforming at the IRS to minimize the total transmit power of the BS under the received user signal-to-noise ratio (SNR) constraints. [17] considered a downlink (DL) multiuser multiple-input single-output (MISO) scenario and maximized the energy efficiency of the BS by alternatively optimizing the transmit beamforming at the BS and the phase shifts at the IRS. Besides, the weighted sum-rate maximization problem for IRS-assisted system was investigated in various scenarios, e.g., MISO system [18], multicell multiple-input multiple-output (MIMO) network [19], and simultaneous wireless information and power transfer (SWIPT) system [20]. The authors in [21] proposed an IRS-assisted mmWAVE communication system in which the IRS is used to overcome the impact of blockage. [22] designed a deep reinforcement learning (DRL)-based algorithm to jointly optimize the active and passive beamforming in the IRS-aided system.

Most of the existing works adopt the IRS to assist either wireless energy transfer (WET) in the DL or wireless information transmission (WIT) in the UL. However, the UL and DL transmissions in WPCNs are highly correlated by the device energy causality. In this sense, a joint design of IRS-assisted DL and UL transmissions is needed to achieve the maximum communication performance in WPCNs. Although this joint design was recently studied in [23], it only considered the optimization of passive beamforming of the IRS in both the DL and UL. The major challenge resides in the joint design of the active beamforming of the HAP and the passive beamforming of the IRS in both DL and UL transmissions. Besides, the user transmit power is affected by both the DL energy transfer and the UL inter-user interference when spatial multiplexing is used. However, to the best of our knowledge, this important research topic has not been studied so far.

In this paper, we study the joint beamforming and user transmit power control problem in an IRS-assisted multiuser

MISO WPCN. As shown in Fig. 1, we consider a multi-antenna half-duplex HAP performing active beamforming to broadcast wireless energy to all WDs in the DL and then receive information transmissions from the WDs in the UL. Specifically, the IRS performs passive beamforming by reflecting the transmitted energy (information) signals in the DL (UL) transmission. During the UL transmission, the WDs perform transmit power control to mitigate the multi-user interference at the HAP. Our objective is to maximize the weighted sum communication rate of all the WDs. The main contributions of this paper are summarized as follows:

- With the proposed IRS-assisted MISO WPCN, we first analyze the achievable data rates of all WDs. Then, we formulate an optimization problem to maximize the weighted sum rate (WSR) of all WDs by jointly optimizing the energy transmission time, the transmit power of the WDs, the active beamforming of the HAP and the passive beamforming of the IRS in both the UL and DL transmissions. The problem is highly non-convex because of the strong coupling of the design variables.
- To tackle this non-convex problem, we first fix the energy transmission time and consider the joint beamforming and user transmit power control problem. Given passive beamforming of the IRS, we convert the remaining active beamforming and transmit power control problem into an equivalent weighted minimum mean square error (WMMSE) problem, which can be efficiently solved by applying a block-coordinate descent (BCD) method. In particular, we show that optimal energy beamforming matrix during the DL energy transfer of the HAP is rank-one and aligned to the maximum eigenmode of the weighted sum of DL channel matrices.
- Given the active beamforming and user transmit power, we then propose a semidefinite relaxation (SDR) method to optimize the passive beamforming of the IRS, including the array reflecting coefficients in both DL and UL transmissions. Accordingly, we devise a block-structured optimization (BSO) technique to update the two sets of variables alternately. Finally, we apply a one-dimensional search method to obtain the optimal energy transmission time.

We conduct extensive simulations to evaluate the performance of the proposed IRS-assisted MISO WPCN. By comparing with the other representative benchmark methods, we show that the proposed method achieves a significant throughput performance gain in multiuser MISO WPCNs.

The rest of the paper is organized as follows: In Section II, we present the system model of the proposed IRS-assisted communication in multiuser MISO WPCN. We formulate the WSR optimization problem in Section III and propose an efficient algorithm to solve it in Section IV. In Section V, we perform simulations to evaluate the performance of the proposed method. Finally, Section VI concludes this paper.

Notations: In this paper, vectors and matrices are denoted by boldface lowercase and uppercase letters, respectively. $\mathbb{C}^{m \times n}$ denotes the space of $m \times n$ complex-valued matrices. The operators $|\cdot|$, $\|\cdot\|$, $(\cdot)^T$ and $(\cdot)^H$ denote the absolute value,

Euclidean norm, transpose and conjugate transpose, respectively. The symbols $\text{tr}(\mathbf{X})$ and $\text{rank}(\mathbf{X})$ denote the trace and rank of matrix \mathbf{X} , respectively. $\mathbb{E}[\cdot]$ stands for the statistical expectation. $\mathcal{CN}(\mu, \sigma^2)$ denotes the distribution of a circularly symmetric complex Gaussian (CSCG) random vector with mean μ and covariance σ^2 . $\mathbf{X} \succeq 0$ means that \mathbf{X} is positive semi-definite. $\arg(\cdot)$ denotes the phase extraction operation and $[\mathbf{x}]_{(1:N)}$ denotes the vector that contains the first N elements of \mathbf{x} . $\text{diag}(\mathbf{x})$ is a diagonal matrix with the entries of the vector \mathbf{x} .

II. SYSTEM MODEL

As shown in Fig. 1, we consider a multiuser MISO WPCN, which consists of one HAP and K WDs. We define the set of WDs as $\mathcal{K} \triangleq \{1, \dots, K\}$. It is assumed that the HAP is equipped with M antennas and each WD has a single antenna. Specifically, the HAP broadcasts wireless energy to the WDs in the DL and receives wireless information transmission from the WDs in the UL. All devices are assumed to operate over the same frequency band, where a time-division-duplexing (TDD) circuit is implemented at both the HAP and the WDs to separate the energy and information transmissions. The HAP performs energy beamforming in the DL and receive beamforming (e.g., MMSE) in the UL information transmission. The HAP has stable power supplies and each WD has an energy harvesting circuit and a rechargeable battery to store the harvested energy to power its operations. To enhance the propagation performance, we employ an IRS composed of N passive elements to assist the transmissions of the WPCN. The IRS can dynamically adjust the phase shift of each reflecting element based on the propagation environment [24]. Due to the substantial path loss, we only consider one-time signal reflection by the IRS and ignore the signals that are reflected thereafter [16].

We assume that all channels follow a quasi-static flat fading model, where all the channel coefficients remain constant during each block transmission time, denoted by T , but vary from block to block. The baseband equivalent channels of HAP-to-IRS, IRS-to-WD $_i$, and HAP-to-WD $_i$ links are denoted as $\mathbf{G} \in \mathbb{C}^{M \times N}$, $\mathbf{g}_i \in \mathbb{C}^{N \times 1}$ and $\mathbf{a}_i \in \mathbb{C}^{M \times 1}, \forall i \in \mathcal{K}$, respectively. It is assumed that the channels of different transceiver pairs are independent to each other. Besides, the entries inside all channel vectors are modeled as zero-mean independent and identically distributed (i.i.d.) complex Gaussian random variables with variance depending on the path loss of the respective wireless links. The corresponding channel gains are denoted as $g_0 = \|\mathbf{G}\|^2$, $g_i = \|\mathbf{g}_i\|^2$ and $h_i = \|\mathbf{a}_i\|^2$. With the IRS-aided channel, each element at the IRS first combines all the received multi-path signals and then re-scatters the combined signal with a certain phase shift. Let $\boldsymbol{\theta} = [\theta_1, \theta_2, \dots, \theta_N]$ and $\boldsymbol{\Theta} = \text{diag}(\beta e^{j\theta_1}, \dots, \beta e^{j\theta_n}, \dots, \beta e^{j\theta_N})$ denote the phase-shift matrix of the IRS, where $\theta_n \in [0, 2\pi]$ and $\beta \in [0, 1]$ are the phase shift and amplitude reflection coefficient of each element, respectively. In this paper, we set $\beta = 1$ for simplicity of in the following analysis, i.e., $\boldsymbol{\Theta} = \text{diag}(v_1, \dots, v_n, \dots, v_N)$ with $|v_n| = 1, n = 1, \dots, N$, and use transmit power control to mitigate the inter-user interference in the UL information transmission.

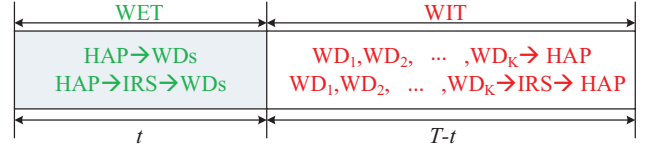


Fig. 2. The transmit protocol of the proposed IRS-assisted MISO WPCN.

As shown in the Fig. 2, we consider a harvest-then-transmit protocol that operates in two phases. In the first phase of duration t , the HAP transfers wireless energy in the DL for all the WDs to harvest. Meanwhile, the IRS scatters the incident signal from the HAP to the WDs, such that the WDs receive signals from both the direct-path and reflect-path channels. The remaining time of the block is assigned for the UL information transmission, during which WDs transmit their independent information to the HAP. Likewise, the IRS simultaneously scatters the signals transmitted by all WDs to the HAP.

We assume that the channel state information (CSI) of all channels are perfectly known at the HAP.¹ We jointly optimize the active beamforming of the HAP and passive beamforming of the IRS in both the UL and DL, the user transmit power, and the transmission time allocation between the UL and DL transmissions, to maximize the WSR of all the users. In the following, we formulate the WSR maximization problem and propose an efficient method to solve it.

III. PROBLEM FORMULATION

In this section, we derive the throughput of each WD and formulate the WSR maximization problem.

A. Phase I: Energy Transfer

In the first WET stage of duration t , we denote $\mathbf{x}(t) \in \mathbb{C}^{M \times 1}$ as the pseudo-random baseband energy signal transmitted by the HAP [2]. The transmit power is constrained by

$$\mathbb{E} [|\mathbf{x}(t)|^2] = \text{tr} (\mathbb{E} [\mathbf{x}(t)\mathbf{x}(t)^H]) \triangleq \text{tr}(\mathbf{W}) \leq P_0. \quad (1)$$

where $\mathbf{W} \succeq 0$ is the energy beamforming matrix, and P_0 denotes the maximum transmit power.

Then, the received signal by the i -th WD is expressed as [16]

$$y_i^{(1)}(t) = (\mathbf{G}\boldsymbol{\Theta}_1\mathbf{g}_i + \mathbf{a}_i)^T \mathbf{x}(t) + n_i(t), \forall i \in \mathcal{K}, \quad (2)$$

where $\boldsymbol{\Theta}_1 = \text{diag}(v_{1,1}, \dots, v_{1,N})$ denotes the energy reflection coefficient matrix at the IRS with $v_{1,n} = e^{j\theta_{1,n}}, n = 1, \dots, N$, which satisfies $|v_{1,n}| = 1$. $n_i(t)$ denotes additive white Gaussian noise (AWGN) at the receiver with $n_i(t) \sim \mathcal{CN}(0, N_0)$.

By neglecting the noise power, the amount of energy harvested by the i -th WD is

$$E_i^{(1)} = \eta \text{tr} \left((\mathbf{G}\boldsymbol{\Theta}_1\mathbf{g}_i + \mathbf{a}_i)(\mathbf{G}\boldsymbol{\Theta}_1\mathbf{g}_i + \mathbf{a}_i)^H \mathbf{W} \right) t, \forall i \in \mathcal{K}, \quad (3)$$

¹The CSI can be precisely estimated by the channel estimation methods for IRS system proposed in [25] and [26], which is out of the scope of this paper.

where $0 < \eta < 1$ denotes the fixed energy harvesting efficiency for all the WDs.² Accordingly, the residual energy of the i -th WD is

$$E_i = \min \{E_0 + E_i^{(1)}, E_{max}\}, \forall i \in \mathcal{K}, \quad (4)$$

where E_0 is the known residual energy at the beginning of the current time slot, and E_{max} is the battery capacity.

B. Phase II: Information Transmission

In the subsequent WIT phase of duration $T - t$, all WDs transmit their independent information simultaneously to the HAP using the harvested energy in phase I. Meanwhile, the IRS reflects signal of the WDs to the HAP. Let $s_i(t)$ denote the information signal transmitted by the i -th WD with $E[|s_i(t)|^2] = 1$, and P_i denote the transmit power of WD $_i$, which is restricted by

$$(T - t)P_i + E_i^{(2)} \leq E_i, \forall i \in \mathcal{K}, \quad (5)$$

where $E_i^{(2)} \geq 0$ denotes the fixed energy consumption of WD $_i$ within a transmission block, such as the data processing unit and passive circuitry power consumption.

Then, the received signals at the HAP from the i -th WD in the UL is

$$\mathbf{y}_i^{(2)}(t) = (\mathbf{G}\Theta_2\mathbf{g}_i + \mathbf{a}_i)\sqrt{P_i}s_i(t) + \sum_{j \in \mathcal{K} \setminus i} (\mathbf{G}\Theta_2\mathbf{g}_j + \mathbf{a}_j)\sqrt{P_j}s_j(t) + \mathbf{n}_0(t), \forall i \in \mathcal{K}, \quad (6)$$

where $\Theta_2 = \text{diag}(v_{2,1}, \dots, v_{2,N})$ denotes the reflection-coefficient matrix at the IRS with $|v_{2,n}| = 1, n = 1, \dots, N$. $\mathbf{n}_0(t) \in \mathbb{C}^{M \times 1}$ denotes the AWGN vector at the HAP with $\mathbf{n}_0(t) \sim \mathcal{CN}(\mathbf{0}, N_0\mathbf{I})$.

It is assumed that the signals of different users are independent. In this paper, we consider linear receive beamforming at the HAP by treating the interference as noise. The estimated signal is expressed as

$$\hat{s}_i = \mathbf{f}_i^H \mathbf{y}_i^{(2)}(t), \forall i \in \mathcal{K}, \quad (7)$$

where $\mathbf{f}_i \in \mathbb{C}^{M \times 1}$ denotes the receiver beamforming vector.

Then, the interference-plus-noise ratio (SINR) at the HAP for decoding the signal of the i -th WD is

$$\gamma_i = \frac{\|\mathbf{f}_i^H(\mathbf{G}\Theta_2\mathbf{g}_i + \mathbf{a}_i)\|^2 P_i}{\sum_{j \in \mathcal{K} \setminus i} \|\mathbf{f}_i^H(\mathbf{G}\Theta_2\mathbf{g}_j + \mathbf{a}_j)\|^2 P_j + \|\mathbf{f}_i^H\|^2 N_0}, \quad \forall i \in \mathcal{K}. \quad (8)$$

Thus, the achievable rate for information transmission of WD $_i$ in the UL is given by

$$R_i = \frac{T - t}{T} \log_2(1 + \gamma_i), \forall i \in \mathcal{K}. \quad (9)$$

where it is assumed without loss of generality that $T = 1$, such that T is not present in the data rate expressions in

²Although a single energy harvesting circuit exhibits non-linear energy harvesting property due to the saturation effect of circuit, it is shown in [27] and [28] that the non-linear effect is effectively rectified by using multiple energy harvesting circuits concatenated in parallel, resulting in a sufficiently large linear conversion region.

the remainder of this paper. Note that a trade-off exists in the WET duration t to maximize R_i . Specifically, a larger t leads to higher allowable transmit power but shorter remaining information transmission time.

C. Problem Formulation

In this paper, we focus on maximizing the WSR of the K WDs by jointly optimizing the transmit time t , user transmit power $\mathbf{P} = [P_1, \dots, P_K]$, the active beamforming of the HAP (including the energy beamforming matrix \mathbf{W} and the receiver beamforming matrix $\mathbf{F} = [\mathbf{f}_1, \dots, \mathbf{f}_K]$), and the passive beamforming of the IRS (i.e., the phase shift matrices Θ_1, Θ_2). Mathematically, it is formulated as

$$\begin{aligned} \text{(P1)} : \quad & \max_{t, \mathbf{P}, \mathbf{W}, \mathbf{F}, \Theta_1, \Theta_2} \sum_{i \in \mathcal{K}} \omega_i R_i \\ \text{s. t.} \quad & (1), (3), (4) \text{ and } (5), \\ & t, P_i \geq 0, \forall i \in \mathcal{K}, \\ & |v_{i,n}| = 1, i = 1, 2, n = 1, \dots, N. \end{aligned} \quad (10)$$

where $\omega_i \geq 0$ is the weighting factor controlling the scheduling priority of WD $_i$.

Notice that the objective function in (9) is not a concave function in the optimizing variables. Besides, due to the modulus constraints and the multiplicative terms of (3), (4) and (5), (P1) is highly non-convex in its current form. In the next section, we first transform (P1) into an equivalent problem and propose an efficient optimization algorithm to solve it.

IV. PROPOSED SOLUTION TO (P1)

We first fix $t = \bar{t}$ in (P1), partition the remaining optimization variables into two blocks, and alternatively optimize the two blocks of variables in an iterative manner [29]. Specifically, the optimization variables are partitioned as $\{\mathbf{W}, \mathbf{F}, \mathbf{P}\}$ and $\{\Theta_1, \Theta_2\}$. Then, we propose efficient algorithms to solve the joint active beamforming and transmit power control subproblem (to optimize $\{\mathbf{W}, \mathbf{F}, \mathbf{P}\}$) and passive beamforming problem (to optimize $\{\Theta_1, \Theta_2\}$) separately in the following.

By assuming that the information messages of different users are independent, i.e., $E[s_i s_j] = 0$ if $i \neq j$, we write the mean-square error (MSE) as

$$\begin{aligned} e_i &= \mathbb{E}_{s_i} \{|\hat{s}_i - s_i|^2\} \\ &= |\mathbf{f}_i^H(\mathbf{G}\Theta_2\mathbf{g}_i + \mathbf{a}_i)\sqrt{P_i} - 1|^2 \\ &\quad + \sum_{j \in \mathcal{K} \setminus i} |\mathbf{f}_i^H(\mathbf{G}\Theta_2\mathbf{g}_j + \mathbf{a}_j)|^2 P_j + N_0 \|\mathbf{f}_i^H\|^2, \forall i \in \mathcal{K}. \end{aligned} \quad (11)$$

Following the celebrated rate-MMSE equivalence established in [30], we show in the following proposition that the original maximization problem can be transformed to a more tractable optimization problem.

Proposition 1: Given $t = \bar{t}$, the WSR maximization problem is equivalent to the following WMMSE problem,

$$(P2) : \min_{\mathbf{W}, \mathbf{F}, \mathbf{P}, \mathbf{q}, \Theta_1, \Theta_2} \sum_{i \in \mathcal{K}} \omega_i (1 - \bar{t}) \left(q_i e_i - \log(q_i) - 1 \right) \quad (12)$$

s. t. (1), (3), (4) and (5),
 $P_i, q_i \geq 0, \forall i \in \mathcal{K}$,
 $|v_{i,n}| = 1, i = 1, 2, n = 1, \dots, N$,

where $\mathbf{q} = [q_1, \dots, q_K]$ and q_i is a positive weight variable for $i = 1 \dots, K$.

Proof: Please refer to Appendix 1.

With the above transformation, we design an efficient alternating optimization algorithm to solve the active beamforming and transmit power control sub-problem described as follows.

A. Optimizing the active beamforming matrices and transmit power $\{\mathbf{W}, \mathbf{F}, \mathbf{P}\}$

We first optimize $\{\mathbf{W}, \mathbf{F}, \mathbf{P}\}$ under fixed Θ_1 and Θ_2 . Define $\mathbf{b}_i = \mathbf{G}\Theta_1 \mathbf{g}_i + \mathbf{a}_i$ and $\tilde{\mathbf{b}}_i = \mathbf{G}\Theta_2 \mathbf{g}_i + \mathbf{a}_i, \forall i \in \mathcal{K}$. Then, (3) and (8) are respectively expressed as,

$$E_i^{(1)} = \eta \text{tr}(\mathbf{b}_i \mathbf{b}_i^H \mathbf{W}) \bar{t}, \forall i \in \mathcal{K}, \quad (13)$$

$$\gamma_i = \frac{\|\mathbf{f}_i^H \tilde{\mathbf{b}}_i\|^2 P_i}{\sum_{j \in \mathcal{K} \setminus i} \|\mathbf{f}_i^H \tilde{\mathbf{b}}_j\|^2 P_j + \|\mathbf{f}_i^H\|^2 N_0}, \forall i \in \mathcal{K}. \quad (14)$$

Accordingly, we reformulate problem (P2) into the following equivalent problem

$$(P3) : \min_{\mathbf{F}, \mathbf{W}, \mathbf{P}, \mathbf{q}} \sum_{i \in \mathcal{K}} \omega_i (1 - \bar{t}) \left(q_i e_i - \log(q_i) - 1 \right) \quad (15)$$

s. t. (1), (4), (5) and (13),
 $P_i, q_i \geq 0, \forall i \in \mathcal{K}$,

where e_i is re-written as

$$e_i = |\mathbf{f}_i^H \tilde{\mathbf{b}}_i \sqrt{P_i} - 1|^2 + \sum_{j \in \mathcal{K} \setminus i} |\mathbf{f}_i^H \tilde{\mathbf{b}}_j|^2 P_j + N_0 \|\mathbf{f}_i^H\|^2. \quad (16)$$

Note that the objective function of problem (P3) is convex over each of the optimization variable \mathbf{f}_i , P_i and q_i for all $i \in \mathcal{K}$. Following [30], we employ a block-coordinate descent (BCD) approach to tackle this problem. Specifically, we optimize one of the block variables in $\{\mathbf{f}_i, P_i, q_i\}$ with the other two fixed. To obtain some insights on the optimal solution structure, we apply the Lagrange duality method to solve (P3). The partial Lagrangian of problem (15) is formulated as

$$\mathcal{L}(\mathbf{F}, \mathbf{W}, \mathbf{P}, \mathbf{q}, \boldsymbol{\mu}) = (1 - \bar{t}) \sum_{i \in \mathcal{K}} \omega_i \left(q_i e_i - \log(q_i) - 1 \right) + \sum_{i \in \mathcal{K}} \mu_i \left((1 - \bar{t}) P_i + E_i^{(2)} \right) - \mu_0 P_0 - \text{tr}(\mathbf{A}\mathbf{W}), \quad (17)$$

where $\mathbf{A} = \sum_{i \in \mathcal{K}} \mu_i \eta \bar{t} \mathbf{b}_i \mathbf{b}_i^H - \mu_0 \mathbf{I}$, μ_0 and $\mu_i, \forall i \in \mathcal{K}$ are the nonnegative dual variables corresponding to the constraints

(1) and (5), respectively. For convenience, we denote $\boldsymbol{\mu} = [\mu_0, \mu_1, \dots, \mu_K]$. Then, the dual function of (P3) is

$$d(\boldsymbol{\mu}) = \min_{\mathbf{F}, \mathbf{W}, \mathbf{P}, \mathbf{q}} \mathcal{L}(\mathbf{F}, \mathbf{W}, \mathbf{P}, \mathbf{q}, \boldsymbol{\mu}) \quad (18)$$

s. t. $\mathbf{F}, \mathbf{W} \succeq 0, \mathbf{P}, \mathbf{q} \geq 0$.

and the dual problem is

$$(P3a) : \max_{\boldsymbol{\mu}} d(\boldsymbol{\mu}) \quad (19)$$

s. t. $\boldsymbol{\mu} \geq 0$.

Therefore, we first investigate the optimal solution of the dual function in (18) given a set of dual variables. Secondly, we determine the optimal dual variables μ_0^* and $\mu_i^*, \forall i \in \mathcal{K}$ to maximize the dual function.

Proposition 2: The optimal energy beamforming matrix \mathbf{W}^* for problem (P3) is expressed as

$$\mathbf{W}^* = P_0 \mathbf{u}_1 \mathbf{u}_1^H. \quad (20)$$

where \mathbf{u}_1 is the unit-norm eigenvector of a matrix $\mathbf{B} = \sum_{i \in \mathcal{K}} \mu_i^* \eta \bar{t} \mathbf{b}_i \mathbf{b}_i^H$ corresponding to the maximum eigenvalue λ_1 . Moreover, the optimal dual variables must satisfy $\mu_i^* > 0$ for $i = 1, \dots, K$ and $\mu_0^* = \lambda_1$.

Proof: Please refer to Appendix 2.

Remark 1: Note that the optimal energy matrix in (20) is rank-one such that transmitting a single energy stream is the optimal strategy for the DL energy transfer. Besides, \mathbf{u}_1 is aligned with the maximum eigenmode of matrix \mathbf{B} . Accordingly, the optimal energy signal $\mathbf{x}(t)$ is determined as $\mathbf{x}(t) = \sqrt{P_0} \mathbf{u}_1 x(t)$, where $x(t)$ denotes an arbitrary random scalar with unit variance.

Furthermore, by checking the first-order optimality conditions for maximizing dual function with respect to q_i , \mathbf{f}_i and P_i , respectively, we have

$$e_i - \frac{1}{q_i} = 0, \quad (21)$$

$$\sum_{j \in \mathcal{K}} 2 \mathbf{f}_i^H \|\tilde{\mathbf{b}}_j\|^2 P_j - 2 \tilde{\mathbf{b}}_i^H \sqrt{P_i} + 2 N_0 \mathbf{f}_i^H = \mathbf{0}, \quad (22)$$

$$\sum_{j \in \mathcal{K}} \omega_j q_j |\mathbf{f}_j^H \tilde{\mathbf{b}}_i|^2 - \frac{\omega_i q_i \mathbf{f}_i^H \tilde{\mathbf{b}}_i}{\sqrt{P_i}} + \mu_i = 0, \quad (23)$$

for all $i \in \mathcal{K}$. Then, we update each block variable in a closed-form manner given by

$$q_i^* = \frac{1}{e_i}, \forall i \in \mathcal{K}, \quad (24)$$

$$\mathbf{f}_i^* = \frac{\tilde{\mathbf{b}}_i \sqrt{P_i}}{\sum_{j \in \mathcal{K}} \|\tilde{\mathbf{b}}_j\|^2 P_j + N_0}, \forall i \in \mathcal{K}, \quad (25)$$

$$P_i^* = \left(\frac{\omega_i q_i \mathbf{f}_i^H \tilde{\mathbf{b}}_i}{\sum_{j \in \mathcal{K}} \omega_j q_j |\mathbf{f}_j^H \tilde{\mathbf{b}}_i|^2 + \mu_i^*} \right)^2, \forall i \in \mathcal{K}. \quad (26)$$

After solving the dual function, we obtain the optimal dual variables μ_i^* by sub-gradient based algorithms, e.g., the ellipsoid method. The subgradient of $d(\boldsymbol{\lambda})$ is denoted as $\boldsymbol{\varsigma} = [\varsigma_1, \dots, \varsigma_K]$, where

$$\varsigma_i = (1 - \bar{t}) P_i^* + E_i^{(2)} - \eta \text{tr}(\mathbf{b}_i \mathbf{b}_i^H \mathbf{W}^*) \bar{t}, \forall i \in \mathcal{K}. \quad (27)$$

The detailed description of the BCD method for problem (P3) is summarized in Algorithm 1.

Algorithm 1: Proposed BCD method for problem (P3)

Input: $P_0, \mathbf{G}, t, \Theta_1, \Theta_2, N_0, \{\mathbf{g}_i, h_i, \forall i \in \mathcal{K}\}$;
Output: $\mathbf{q}^*, \mathbf{P}^*, \mathbf{W}^*, \mathbf{F}^*$;
 1 **Initialize:** $j \leftarrow 0, \boldsymbol{\mu}^{(0)} > 0$, feasible $\mathbf{q}^{(0)}, \mathbf{F}^{(0)}, \mathbf{P}^{(0)}$;
 2 **repeat**
 3 Calculate $\mathbf{W}^{(j+1)}$ using (20) with given $\boldsymbol{\mu}^{(j)}$;
 4 Calculate e_i in (16) with given $\mathbf{f}_i^{(j)}$ and $P_i^{(j)}$;
 5 Calculate $q_i^{(j+1)}$ using (24) with given $\mathbf{f}_i^{(j)}$ and $P_i^{(j)}$;
 6 Calculate $\mathbf{f}_i^{(j+1)}$ using (25) with given $q_i^{(j+1)}$ and $P_i^{(j)}$;
 7 Calculate $P_i^{(j+1)}$ using (26) with given $q_i^{(j+1)}$ and $\mathbf{f}_i^{(j+1)}$;
 8 Calculate the sub-gradient of $\boldsymbol{\mu}^{(j)}$ using (27);
 9 Update $\boldsymbol{\mu}^{(j+1)}$ by using the ellipsoid method;
 10 $j \leftarrow j + 1$;
 11 **until** The optimal objective value of primal problem (P3) converges;
 12 **Return** $\{\mathbf{q}^*, \mathbf{P}^*, \mathbf{W}^*, \mathbf{F}^*\}$ as a solution to (P3).

B. Optimizing the passive beamforming matrices $\{\Theta_1, \Theta_2\}$

Now, we optimize the phase shift matrices $\{\Theta_1, \Theta_2\}$ given fixed $\{\mathbf{W}, \mathbf{F}, \mathbf{P}\}$. Let $\mathbf{v}_n = [v_{n,1}, \dots, v_{n,N}]^T, n = 1, 2$. Define $\zeta_i = \mathbf{G} \text{diag}(\mathbf{g}_i^T) \in \mathbb{C}^{M \times N}, \forall i \in \mathcal{K}$. Then, we have

$$\begin{aligned} \mathbf{G}\Theta_n \mathbf{g}_i + \mathbf{a}_i &= \mathbf{G} \text{diag}(\mathbf{g}_i^T) \mathbf{v}_n + \mathbf{a}_i \\ &= \zeta_i \mathbf{v}_n + \mathbf{a}_i. \end{aligned} \quad (28)$$

To tackle the non-convex modulus constraint in (P2), we first define $\bar{\mathbf{v}}_n = \begin{bmatrix} \mathbf{v}_n \\ 1 \end{bmatrix} \in \mathbb{C}^{(N+1) \times 1}, n = 1, 2, \bar{\zeta}_i = [\zeta_i, \mathbf{a}_i] \in \mathbb{C}^{M \times (N+1)}$ and $\mathbf{V}_n = \bar{\mathbf{v}}_n \bar{\mathbf{v}}_n^H \in \mathbb{C}^{(N+1) \times (N+1)}$. Thus, we have

$$\begin{aligned} \|\mathbf{f}_i^H (\mathbf{G}\Theta_2 \mathbf{g}_i + \mathbf{a}_i)\|^2 &= \|\mathbf{f}_i^H (\zeta_i \mathbf{v}_2 + \mathbf{a}_i)\|^2 \\ &= \|\mathbf{f}_i^H \bar{\zeta}_i \bar{\mathbf{v}}_2\|^2 = \text{tr}(\mathbf{V}_2 \bar{\zeta}_i^H \mathbf{f}_i \mathbf{f}_i^H \bar{\zeta}_i). \end{aligned} \quad (29)$$

Accordingly, we rewrite (3) as

$$E_i^{(1)} = \eta \bar{t} \text{tr}(\mathbf{V}_1 \bar{\zeta}_i^H \mathbf{W} \bar{\zeta}_i), \forall i \in \mathcal{K}. \quad (30)$$

Consider the following transformation

$$\begin{aligned} &|\mathbf{f}_i^H (\mathbf{G}\Theta_2 \mathbf{g}_i + \mathbf{a}_i) \sqrt{P_i} - 1|^2 \\ &= |\mathbf{f}_i^H (\zeta_i \mathbf{v}_2 + \mathbf{a}_i) \sqrt{P_i} - 1|^2 \\ &= |\mathbf{f}_i^H \bar{\zeta}_i \bar{\mathbf{v}}_2 \sqrt{P_i} + \mathbf{f}_i^H \mathbf{a}_i \sqrt{P_i} - 1|^2 \\ &= \|\hat{\zeta}_i \bar{\mathbf{v}}_2\|^2 = \text{tr}(\mathbf{V}_2 \psi_i), \end{aligned} \quad (31)$$

where $\hat{\zeta}_i = [\mathbf{f}_i^H \bar{\zeta}_i \sqrt{P_i}, \mathbf{f}_i^H \mathbf{a}_i \sqrt{P_i} - 1] \in \mathbb{C}^{1 \times (N+1)}$ and $\psi_i = \hat{\zeta}_i^H \bar{\zeta}_i \in \mathbb{C}^{(N+1) \times (N+1)}, \forall i \in \mathcal{K}$. Then, the MSE in (11) is re-expressed as

$$\begin{aligned} e_i(\mathbf{V}) &= |\mathbf{f}_i^H (\mathbf{G}\Theta_2 \mathbf{g}_i + \mathbf{a}_i) \sqrt{P_i} - 1|^2 \\ &+ \sum_{j \in \mathcal{K} \setminus i} |\mathbf{f}_i^H (\mathbf{G}\Theta_2 \mathbf{g}_j + \mathbf{a}_j)|^2 P_j + N_0 \|\mathbf{f}_i^H\|^2 \\ &= \|\hat{\zeta}_i \bar{\mathbf{v}}_2\|^2 + \sum_{j \in \mathcal{K} \setminus i} \|\mathbf{f}_i^H \bar{\zeta}_j \bar{\mathbf{v}}_2\|^2 P_j + N_0 \|\mathbf{f}_i^H\|^2 \\ &= \text{tr}(\mathbf{V}_2 \psi_i) + \sum_{j \in \mathcal{K} \setminus i} \text{tr}(\mathbf{V}_2 \bar{\zeta}_j^H \mathbf{f}_i \mathbf{f}_i^H \bar{\zeta}_j) P_j + N_0 \text{tr}(\mathbf{f}_i \mathbf{f}_i^H). \end{aligned} \quad (32)$$

Note that $[\mathbf{V}_i]_{n,n} = 1, i = 1, 2, n = 1, \dots, N+1$ hold from the modulus constraint of $v_{i,n}$ ($[\mathbf{X}]_{m,n}$ denotes the element

in the m -th row and n -th column of matrix \mathbf{X}). Besides, \mathbf{V}_i must satisfy $\text{rank}(\mathbf{V}_i) = 1$. Thus, we rewrite problem (P2) as

$$\begin{aligned} \text{(P4)} : \quad & \min_{\mathbf{V}_1, \mathbf{V}_2} \sum_{i=1}^K \omega_i (1 - \bar{t}) (q_i e_i(\mathbf{V}) - \log(q_i) - 1) \\ \text{s. t.} \quad & (4), (5) \text{ and } (30), \\ & [\mathbf{V}_i]_{n,n} = 1, i = 1, 2, n = 1, \dots, N+1, \\ & \text{rank}(\mathbf{V}_i) = 1, \mathbf{V}_i \succeq 0. \end{aligned} \quad (33)$$

Dropping the non-convex rank-one constraint and removing the terms irrelevant to $\mathbf{V}_1, \mathbf{V}_2$, we reduce problem (P4) to

$$\begin{aligned} \text{(P4a)} : \quad & \min_{\mathbf{V}_1, \mathbf{V}_2 \succeq 0} \sum_{i=1}^K \omega_i q_i e_i(\mathbf{V}) \\ \text{s. t.} \quad & (4), (5) \text{ and } (30) \\ & [\mathbf{V}_i]_{n,n} = 1, i = 1, 2, n = 1, \dots, N+1. \end{aligned} \quad (34)$$

Note that problem (P4a) is a standard semidefinite programming (SDP) and it can be efficiently solved by the optimization tools such as CVX [31]. Let's denote the optimal solution to problem (P4a) as $\{\mathbf{V}_1^*, \mathbf{V}_2^*\}$. Generally, the relaxed problem (P4a) may not yield a rank-one solution. To recover \mathbf{v}_i from \mathbf{V}_i^* for $i = 1, 2$, we obtain the eigenvalue decomposition of \mathbf{V}_i^* as $\mathbf{V}_i^* = \mathbf{U}_i \boldsymbol{\Sigma}_i \mathbf{U}_i^H$, where $\mathbf{U}_i \in \mathbb{C}^{(N+1) \times (N+1)}$ and $\boldsymbol{\Sigma}_i \in \mathbb{C}^{(N+1) \times (N+1)}$ denote a unitary matrix and diagonal matrix, respectively. Then, we apply the standard Gaussian randomization method [32] to obtain a suboptimal solution $\bar{\mathbf{v}}_i$, i.e., $\bar{\mathbf{v}}_i = \mathbf{U}_i \boldsymbol{\Sigma}_i^{1/2} \mathbf{r}_i, i = 1, 2$, where $\mathbf{r}_i \in \mathbb{C}^{(N+1) \times 1}$ is a random vector generated from $\mathbf{r}_i \sim \mathcal{CN}(\mathbf{0}, \mathbf{I}_{N+1})$. With many candidate solutions \mathbf{r}_i 's, we select the best one $\bar{\mathbf{v}}_i$ among all \mathbf{r}_i which minimizes the objective of (P4a). Finally, we obtain $\mathbf{v}_i^* = e^{j \arg([\bar{\mathbf{v}}_i]_{(1:N)}/\bar{v}_{i,N+1})}$, the optimal Θ_1^* and Θ_2^* can be obtained from \mathbf{v}_1^* and \mathbf{v}_2^* , respectively.

Algorithm 2: Proposed BSO-based alternating iterative algorithm to problem (P1) with given $t = \bar{t}$

Input: $P_0, N, \mathbf{G}, t, N_0, \{\mathbf{g}_i, h_i, \forall i \in \mathcal{K}\}$;
Output: $\mathbf{P}^*, \mathbf{W}^*, \mathbf{F}^*, \Theta_1^*, \Theta_2^*$;
 1 **Initialize:** $k \leftarrow 0, t \leftarrow \bar{t}, \Theta_1^{(0)}$ and $\Theta_2^{(0)}$;
 2 **repeat**
 3 Calculate $\mathbf{W}^{(k+1)}, \mathbf{F}^{(k+1)}$ and $\mathbf{P}^{(k+1)}$ from Algorithm 1;
 4 Update $\mathbf{V}_i^{(k+1)}$ by solving SDP in (34) and recover $\mathbf{v}_i^{(k+1)}$ ($\Theta_i^{(k+1)}$) from $\mathbf{V}_i^{(k+1)}$;
 5 $k \leftarrow k + 1$;
 6 **until** The optimal objective value of (P1) converges;
 7 **Return** $\{\mathbf{P}^*, \mathbf{W}^*, \mathbf{F}^*, \Theta_1^*, \Theta_2^*\}$ as a solution to (P1).

Based on the solutions to the two sub-problems (P3) and (P4), we devise an efficient iterative algorithm summarized in Algorithm 2. Specifically, given $t = \bar{t}$, the algorithm starts with certain feasible values of $\Theta_1^{(0)}$ and $\Theta_2^{(0)}$. Next, given a fixed solution $\{\Theta_1^{(k)}, \Theta_2^{(k)}\}$ in the k -th iteration, we first obtain the optimal $\mathbf{W}^{(k+1)}, \mathbf{F}^{(k+1)}$ and $\mathbf{P}^{(k+1)}$ from Algorithm 1. Then, we update the phase shift matrices $\Theta_1^{(k+1)}$ and $\Theta_2^{(k+1)}$ using the SDR technique to solve problem (P4a) in the $(k+1)$ -th iteration. The process repeats until convergence. At last, we obtain the optimal energy transmission time t^* via a simple

one-dimensional search method over $t \in (0, 1)$, e.g., golden-section search [33] or the data-driven-based search [34], which is omitted here for brevity.

C. Convergence and Complexity Analysis

The proposed BSO algorithm alternately solves two sub-problems (P3) and (P4) that optimize $\{\mathbf{W}, \mathbf{F}, \mathbf{P}\}$ and $\{\Theta_1, \Theta_2\}$, respectively. Following the Theorem 3 in [30], the BCD method used in Algorithm 1 converges and the objective value of (P3) after optimization is non-increasing compared to that achieved by the initial input parameter. Besides, by our design, the randomization method used to solve (P4a) also guarantees that the objective is non-increasing after optimization. Due to the equivalence in **Proposition 1**, now that the objective of (P1) is non-decreasing in both the alternating steps and the optimal value of (P1) is bounded above, we conclude that the proposed Algorithm 2 converges asymptotically. In a practical setup, we will show the number of alternating iterations consumed by Algorithm 2 until convergence in simulation section.

We then analyze the complexity of Algorithm 2. Here, we consider $N > M \geq K$ in a practical IRS-assisted multiuser MISO WPCN. The complexity of problem (P3) is dominated by the calculation of \mathbf{W}^* , which requires calculating the eigenvalue decomposition of an $M \times M$ matrix \mathbf{B} with complexity of $\mathcal{O}(M^3)$ [35]. The SDP problem (P4a) can be solved with a worst-case complexity of $\mathcal{O}((N+1)^{4.5})$ [36]. As we will show later in Fig. 9, the number of alternating iterations used by Algorithm 2 until convergence is of constant order, i.e., $\mathcal{O}(1)$, regardless of the value of M and N . Therefore, the overall complexity of Algorithm 2 is $\mathcal{O}(M^3 + (N+1)^{4.5})$.

V. SIMULATION RESULTS

In this section, we provide numerical results to evaluate the performance of the proposed IRS-assisted MISO WPCN. In all simulations, we consider a two-dimensional (2D) coordinate system as shown in Fig. 3, where the HAP and IRS are located at $(0, 0)$ and $(4, 3)$, the WDs are uniformly and randomly placed in a circle centered at $(d_c, 0)$ with radius equal to 2 m [23]. To account for the small-scale fading, we assume that all channels follow Rayleigh fading and the distance-dependent path loss is modeled as $L = C_0(\frac{d}{d_0})^{-\alpha}$, where C_0 is the constant path loss at the reference distance d_0 , d denotes the link distance, and α denotes the path loss exponent. To account for the heterogeneous channel conditions and avoid severe signal blockage, we set different path loss exponents of the HAP-IRS, IRS-WD $_i$ and HAP-WD $_i$ channels as 2.0, 2.2 and 3.5, respectively. For simplicity, we assume equal weights $\omega_i = 1$ in all simulations.

Unless otherwise stated, the parameters used in the simulations are listed in Table I, which corresponds to a typical outdoor wireless powered sensor network similar to the setups in [18] and [23]. The number of random vector for Gaussian randomization is set as 100 and the stopping criteria for the proposed algorithm is set as 10^{-4} . All the simulation results are obtained by averaging over 1000 independent channel realizations.

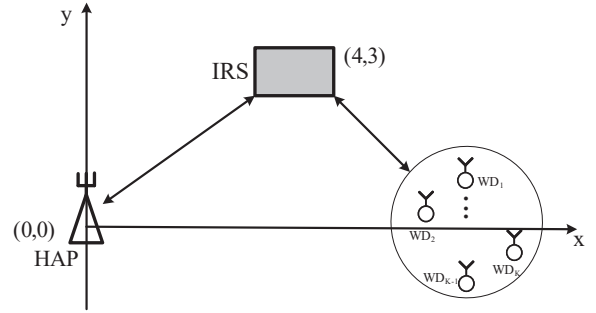


Fig. 3. The placement model of simulation setup.

TABLE I
SYSTEM PARAMETERS

Parameter	Description	Value
P_0	Maximum transmission power of HAP	30 dBm
η	Energy harvesting efficiency	0.8
C_0	Fixed path loss at reference distance	20 dB
N_0	Noise power at receiver antenna	-90 dBm
K	Number of WDs	4
M	Number of HAP antennas	6
N	Number of reflecting elements	30
d_c	Distance between the HAP and WDs	8 m
$E_i^{(2)}$	Circuit energy consumption of WD $_i$	10^{-6} J [37]
ω_i	Weight factor of WD $_i$	1

In addition, we select three representative benchmark methods for performance comparison:

- 1) *Passive beamforming optimization (PBO)*: We set uniform energy beamforming (i.e., $\mathbf{W} = \mathbf{I}_M$) and MMSE receive beamforming in line 3 of Algorithm 2. Then, the user transmit power P_i and passive beamforming of the IRS $\{\Theta_1, \Theta_2\}$ are optimized alternatively in an iterative manner similarly to our proposed method. This method corresponds to the case that optimizes only the passive beamforming of the considered WPCN.
- 2) *Active beamforming optimization (ABO)*: In this case, the phase shifts of all reflecting elements at the IRS for both WET and WIT are fixed and uniformly generated as $\theta_{i,n} \in [0, 2\pi]$. The other variables are optimized using our proposed method. This method corresponds to the case where only the active beamforming of the HAP is optimized.
- 3) *Without IRS*: All WDs first harvest energy from the HAP and then transmit independently to the HAP. This corresponds to the method in [7].

For fair comparison, we optimize the resource allocations in all the benchmark schemes. The details are omitted due to the page limit.

Fig. 4 shows the impact of the maximum transmit power of the HAP (i.e., P_0) to the WSR performance. As expected, the WSR of all schemes increases with P_0 because the WDs are able to harvest more energy when the transmit power of HAP is higher. The joint optimization method achieves evident performance advantage over the other methods. In particular,

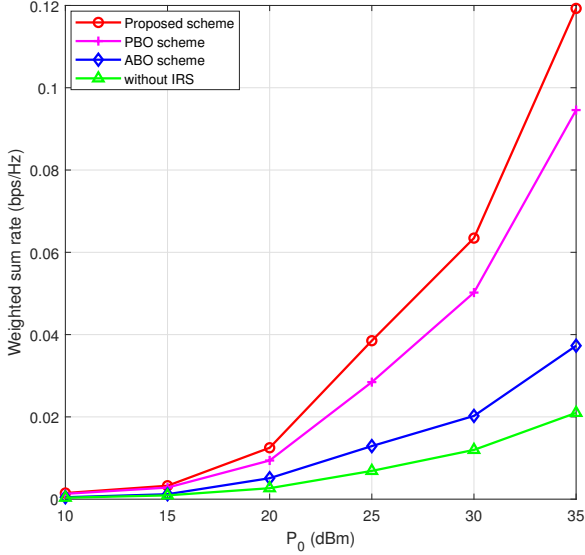


Fig. 4. The WSR performance versus the maximum transmit power of the HAP.

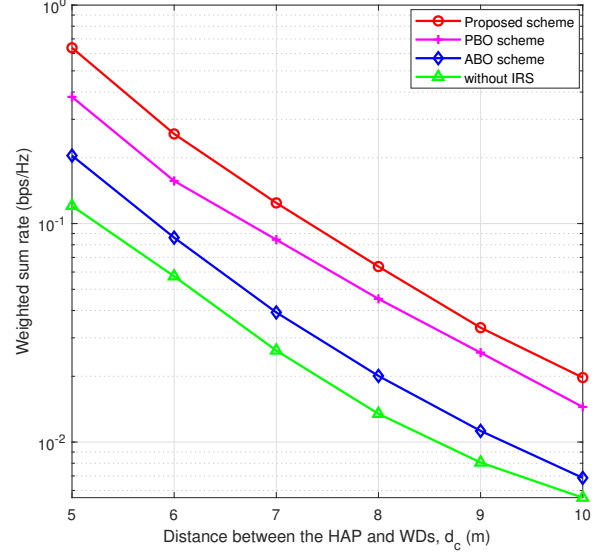


Fig. 6. The WSR performance versus the distance between the HAP and WDs.

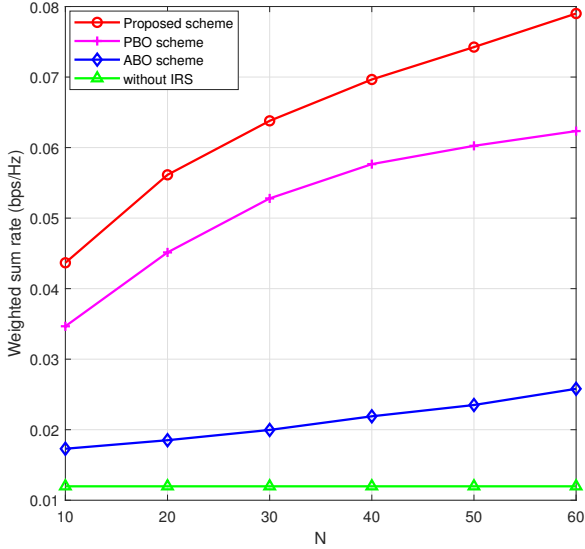


Fig. 5. The WSR performance versus the number of IRS reflecting elements.

the performance gap between the proposed scheme with the benchmark methods increases with P_0 , which demonstrates its efficient usage of the harvested energy. It is also worth mentioning that even the IRS-assisted method with fixed phase shifts achieves better performance than that without the IRS thanks to the array energy gain provided by the IRS.

In Fig. 5, we study the impact of number of reflecting elements N on the WSR performance when the value of N varies from 10 to 60. We observe an evident increase of the WSR for the three IRS-assisted methods. In particular, compared to the ABO scheme, the slope of increase is larger for the proposed scheme and the PBO methods, because they can achieve extra beamforming gain besides the array gain of the IRS. By jointly optimizing the active and passive beamforming, our proposed scheme significantly outperforms

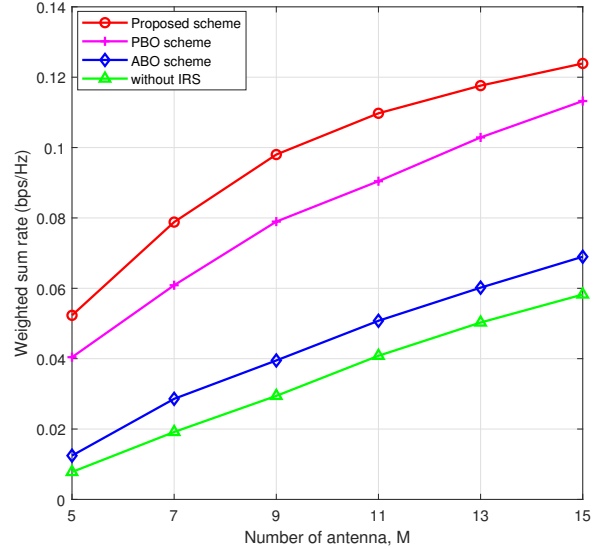


Fig. 7. The WSR performance versus the number of HAP antennas.

the PBO and ABO schemes. On average, the proposed joint optimization method achieves 23.66%, 205.57% and 360.98% higher throughput than the three benchmark methods, respectively.

Fig. 6 investigates the impact of the WDs deployment location to the WSR performance by varying d_c . We also see that the performance gain of all the methods decreases as d_c increases, because as the WDs move further away from both the HAP and IRS, and suffering from more severe signal attenuation in both energy harvesting and information transmission. The performance gain is especially evident when d_c is large, e.g. $d_c > 9$ m, where the without-IRS scheme achieves very low rate (less than 10^{-2}) while the proposed scheme still maintains

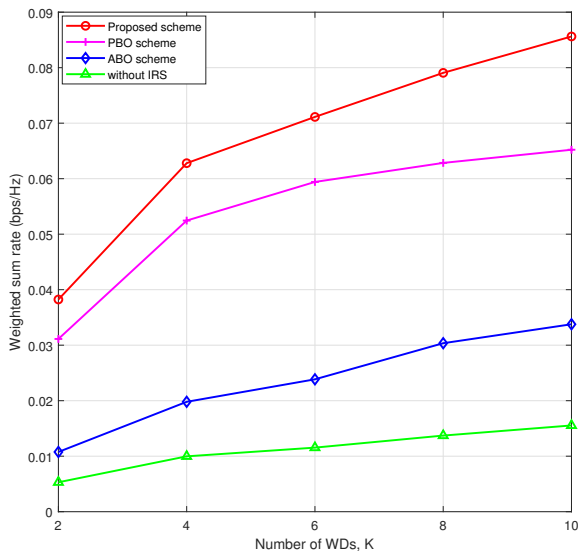


Fig. 8. The WSR performance versus the number of WDs.

relatively high rate (around ten times larger). This is because the WDs are unable to efficiently harvest sufficient energy for information transmission without the assistance of the IRS.

Then, we compare in Fig. 7 the WSR performance of all the schemes when the number of the HAP antennas (i.e., M) changes. It is observed that the WSR performance of all the methods increases with M because of the higher spatial diversity gain. We also notice that our proposed scheme and the PBO scheme produce much better performance than the other two schemes due to the higher beamforming gain. Meanwhile, the performance of ABO scheme even performs close to the without-IRS scheme, which implies the importance of optimizing the passive beamforming to the throughput performance.

In Fig. 8, we evaluate the WSR performance versus the number of WDs (i.e., K) for all the methods. Here, we vary K from 2 to 10. It can be observed that the WSR performance increases with the number of WDs for all methods due to the benefit of multiuser diversity. Meanwhile, the performance gap between the three IRS-assisted methods and the without-IRS scheme gradually increases with K . This is because the uplink information transmission becomes interference-limited when the number of WDs is large. As a result, the optimal solution will allocate more time for transmitting information, which in consequence decreases the WET phase duration. In this case, the IRS becomes a critical factor that effectively increases the harvested energy of the WDs within the limited energy transfer time.

We then show in Fig. 9 the convergence rate of Algorithm 2, for which the convergence is proved in Section IV.C. In particular, we plot the average number of iterations required until the algorithm converges under 100 independent simulations. Here, we investigate the convergence rate when either the number of HAP antennas (i.e., M) or IRS reflecting elements (i.e., N) varies. With fixed $N = 30$ in Fig. 9(a), we see that the number of iterations used till convergence does not vary significantly

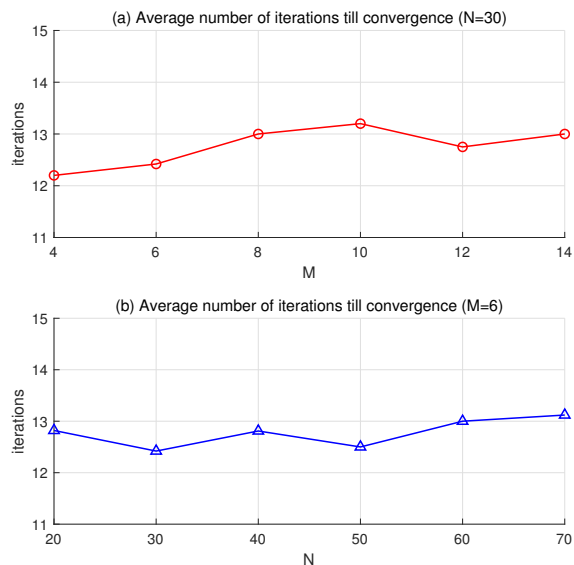


Fig. 9. The average iteration number of convergence of Algorithm 2, (a) as a function of M under fixed $N = 30$; and (b) as a function of N under fixed $M = 6$.

as M increases. Similarly in Fig. 9(b), with a fixed $M = 6$, we do not observe significant increase of iterations when N increases from 20 to 70. Besides, all the simulations performed in Fig. 9 require at most 20 iterations to converge. Therefore, we can safely estimate that the number of iterations used till convergence is of constant order, i.e., $\mathcal{O}(1)$. This indicates that the proposed method enjoys fast convergence even in a network with a large number of active antennas at the HAP or passive reflecting elements at the IRS.

To sum up, our simulation results show that the proposed joint beamforming and power control optimization achieves superior throughput performance in MISO WPCNs under various setups. Meanwhile, we observe that, between the two better performing benchmark method, the PBO method outperforms the ABO scheme in all simulations. This indicates the importance of a refined passive beamforming design to achieve the high beamforming gain provided by the massive reflecting elements. Nonetheless, the significant performance gap between the PBO scheme and our proposed scheme confirms the benefit of joint active and passive beamforming optimization in enhancing the throughput performance of IRS-assisted WPCNs.

VI. CONCLUSIONS AND FUTURE WORK

In this paper, we have studied an IRS-assisted multiuser MISO WPCN. Specifically, the WSR optimization problem was formulated to jointly optimize the energy transmission time, the user transmit power, the active beamforming of the HAP and passive beamforming of IRS in both the UL and DL transmissions. To tackle this non-convex problem, we fixed the passive beamforming of the IRS and converted the original problem to an equivalent WMMSE problem, which was efficiently solved by a BCD method. Likewise, given user transmit power and active beamforming of the HAP, we optimized the passive beamforming of the IRS by the SDR

technique. This leads to a BSO-based iterative algorithm to update the two sets of variables alternately. At last, we applied an one-dimensional search method to obtain the optimal WET time. By comparing with representative benchmark methods, we showed that the proposed joint optimization achieves significant performance advantage and effectively enhances the throughput performance in multi-user MISO WPCNs under different practical network setups.

Finally, we conclude the paper with some interesting future working directions. First, it is interesting to consider a practical non-linear energy harvesting model, such that the active and passive beamforming design in the DL energy transfer must be adapted to improve the energy harvesting efficiency of all users. In addition, it is also promising to consider more realistic imperfect CSI case, where the knowledge of the cascaded HAP-IRS-WD channels are under uncertainty due to channel estimation error. To tackle the problem, we may investigate the robust transmission design for IRS-assisted MISO communication systems under a stochastic CSI error model. Moreover, although some recent works have considered IRS with only a finite number of phase shifts at each element. In this case, the beamforming problem becomes very challenging due to the combinatorial phase shift variables and the strong coupling with the other system design parameters. One possible way is to introduce a learning-based discrete beamforming method for reducing the computational complexity. At last, it is also challenging to extend the considered network model to other practical setups, such as full-duplex transmission, cluster-based cooperation, hardware-constrained reflection at the IRS, and non-interference scenario, etc.

APPENDIX 1

PROOF OF PROPOSITION 1

Proof: Firstly, by employing the well-known rate-MMSE equivalence established in [30], we have

$$\log(1 + \gamma_i) = \log([e_i^{\text{MMSE}}]^{-1}), \quad (35)$$

where e_i^{MMSE} denotes the MMSE of received signal s_i from WD $_i$, and it is expressed as

$$e_i^{\text{MMSE}} = \min e_i, \quad (36)$$

where e_i is defined as (11). Then, by substituting it into (35), we have

$$\log(1 + \gamma_i) = \log([\min e_i]^{-1}) = \max \log(e_i^{-1}). \quad (37)$$

Consider the following equality

$$\log(x^{-1}) = \max_{y \geq 0} (\log(y) - (xy) + 1), \quad (38)$$

where the optimal solution is achieved at $y^* = x^{-1}$. Thus, we rewrite (37) as

$$\begin{aligned} \log(1 + \gamma_i) &= \max \log(e_i^{-1}) \\ &= \max_{q_i \geq 0} (\log(q_i) - (q_i e_i) + 1) \\ &= \min_{q_i \geq 0} ((q_i e_i) - \log(q_i) - 1). \end{aligned} \quad (39)$$

Accordingly, given $t = \bar{t}$, problem (P1) can be transformed into the equivalent problem as (P2).

APPENDIX 2

PROOF OF PROPOSITION 2

Proof: The Karush-Kuhn-Tucker (KKT) conditions of (P3) with respect to \mathbf{W}^* are

$$\bar{\mathbf{A}} \mathbf{W}^* = \mathbf{0}, \quad (40)$$

$$\mu_i^* \geq 0, \mu_0^* \geq 0, \mathbf{W}^* \succeq \mathbf{0}, \forall i \in \mathcal{K}, \quad (41)$$

$$\mu_0^* (\text{tr}(\mathbf{W}^*) - P_0) = 0, \quad (42)$$

$$\mu_i^* ((1 - \bar{t})P_i + E_i^{(2)} - \eta \bar{t} \text{tr}(\mathbf{b}_i \mathbf{b}_i^H \mathbf{W}^*)) = 0, \forall i \in \mathcal{K}, \quad (43)$$

where $\bar{\mathbf{A}} = \sum_{i \in \mathcal{K}} \mu_i^* \eta \bar{t} \mathbf{b}_i \mathbf{b}_i^H - \mu_0^* \mathbf{I}$.

In practice, we always find a rank-one energy beamforming matrix by using the derived optimal conditions in (40)-(43). We first consider the case of $\mu_i^* = 0$ and $\mu_0^* > 0$. In this case, we have $\mathbf{W}^* = \mathbf{0}$ from (40) since $\bar{\mathbf{A}} = -\mu_0^* \mathbf{I}$, which contradicts the complementary slackness condition (42). Also, for the case where $\mu_i^* > 0$ and $\mu_0^* = 0$, $\mathbf{W}^* = \mathbf{0}$ from (40) since $\bar{\mathbf{A}} = \sum_{i \in \mathcal{K}} \mu_i^* \eta \bar{t} \mathbf{b}_i \mathbf{b}_i^H$, which contradicts the complementary slackness condition (43). Hence, both μ_0^* and μ_i^* are greater than zero, i.e., $\mu_0^* > 0$ and $\mu_i^* > 0$, $\forall i \in \mathcal{K}$.

Next, we denote $\mathbf{B} = \sum_{i \in \mathcal{K}} \mu_i^* \eta \bar{t} \mathbf{b}_i \mathbf{b}_i^H$. Let the eigenvalue decomposition of matrix $\bar{\mathbf{A}}$ be $\bar{\mathbf{A}} = \mathbf{U}(\mathbf{\Lambda} - \mu_0^* \mathbf{I})\mathbf{U}^H$, where $\mathbf{U} \in \mathbb{C}^{M \times M}$ and $\mathbf{\Lambda} = \text{diag}(\lambda_1, \dots, \lambda_M) \in \mathbb{C}^{M \times M}$ with $\lambda_1 \geq \dots \geq \lambda_M$ are the eigenvector matrix and eigenvalue matrix of \mathbf{B} , respectively. Since $\mu_i^* > 0$, $\forall i \in \mathcal{K}$, \mathbf{B} is always a positive semidefinite, and resulting in the non-negative eigenvalues λ_j , for $j = 1, \dots, M$. Thus, for $\bar{\mathbf{A}}$ to have non-positive eigenvalues, i.e., $\lambda_j - \mu_0^* \leq 0$, we obtain $0 \leq \lambda_j \leq \mu_0^*$. When $\mu_i^* > 0$, $\forall i \in \mathcal{K}$, we have $\text{rank}(\mathbf{B}) > 1$, the maximum eigenvalue $\lambda_1 > 0$.

Note that if $\mu_0^* > \lambda_1$, $\bar{\mathbf{A}}$ becomes a full-rank and negative-definite matrix. Thus, we obtain $\mathbf{W} = \mathbf{0}$ from (40), which contradicts the complementary slackness condition (42) since $\mu_0^* > 0$. Therefore, we obtain the optimal dual variable μ_0^* as $\mu_0^* = \lambda_1$. We define $\bar{\mathbf{A}} \mathbf{u}_1 = \mathbf{0}$, where \mathbf{u}_1 is the unit-norm eigenvector of \mathbf{B} corresponding to the maximum eigenvalue λ_1 . From (40) and (41), we obtain the optimal $\mathbf{W}^* = \epsilon \mathbf{u}_1 \mathbf{u}_1^H$ for any $\epsilon \geq 0$. Next, we find ϵ from (42), i.e., $P_0 - \text{tr}(\mathbf{W}^*) = 0$ due to $\mu_0^* > 0$, which leads to $\text{tr}(\mathbf{W}^*) = \epsilon = P_0$. ■

REFERENCES

- [1] L. Chettri and R. Bera, "A comprehensive survey on Internet of Things (IoT) toward 5G wireless systems," *IEEE Internet Things J.*, vol. 7, no. 1, pp. 16-32, Jan. 2020.
- [2] S. Bi, C. K. Ho, and R. Zhang, "Wireless powered communication: Opportunities and challenges," *IEEE Commun. Mag.*, vol. 53, no. 4, pp. 117-125, Apr. 2015.
- [3] S. Bi and Y. J. Zhang, "Computation rate maximization for wireless powered mobile-edge computing with binary computation offloading," *IEEE Trans. Wireless Commun.*, vol. 17, no. 6, pp. 4177-4190, Jun. 2018.
- [4] L. Huang, S. Bi, and Y. J. Zhang, "Deep reinforcement learning for online computation offloading in wireless powered mobile-edge computing networks," *IEEE Trans. Mobile Comput.*, vol. 19, no. 11, pp. 2581-2593, Nov. 2020.
- [5] H. Ju and R. Zhang, "User cooperation in wireless powered communication networks," in *Proc. IEEE Global Commun. Conf. (GLOBECOM)*, Austin, TX, USA, Dec. 2014, pp. 1430-1435.
- [6] Y. Zheng, S. Bi, X. Lin, and H. Wang, "Reusing wireless power transfer for backscatter-assisted relaying in WPCNs," *Comput. Netw.*, vol. 175, pp. 1-12, Jul. 2020.

- [7] L. Liu, R. Zhang, and K.-C. Chua, "Multi-antenna wireless powered communication with energy beamforming," *IEEE Trans. Commun.*, vol. 62, no. 12, pp. 4349-4361, Dec. 2014.
- [8] C. Huang, S. Hu, G. C. Alexandropoulos, A. Zappone, C. Yuen, R. Zhang, M. Di. Renzo, and M. Debbah, "Holographic MIMO surfaces for 6G wireless networks: Opportunities, challenges, and trends," *IEEE Wireless Commun.*, vol. 27, no. 5, pp. 118-125, Oct. 2020.
- [9] T. J. Cui, M. Q. Qi, X. Wan, J. Zhao, and Q. Cheng, "Coding metamaterials, digital metamaterials and programmable metamaterials," *Light Sci. & Appl.*, vol. 3, no. 10, p. e218, Oct. 2014.
- [10] Q. Wu and R. Zhang, "Towards smart and reconfigurable environment: Intelligent reflecting surface aided wireless network," *IEEE Commun. Mag.*, vol. 58, no. 1, pp. 106-112, Jan. 2020.
- [11] S. Foo, "Liquid-crystal reconfigurable metasurface reflectors," in *Proc. IEEE Int. Symp. Antennas Propag. USNC/URSI Nat. Radio Sci. Meeting*, San Diego, CA, USA, Jul. 2017, pp. 2069-2070.
- [12] C. Liaskos, S. Nie, A. Tsioliaridou, A. Pitsillides, S. Ioannidis, and I. Akyildiz, "A new wireless communication paradigm through software-controlled metasurfaces," *IEEE Commun. Mag.*, vol. 56, no. 9, pp. 162-169, Sep. 2018.
- [13] W. Zhao, G. Wang, S. Atapattu, T. A. Tsiftsis, and X. Ma, "Performance analysis of large intelligent surface aided backscatter communication systems," *IEEE Wireless Commun. Lett.*, vol. 9, no. 7, pp. 962-966, Jul. 2020.
- [14] J. Yuan, Y.-C. Liang, J. Joung, G. Feng, and E. G. Larsson, "Intelligent reflecting surface-assisted cognitive radio system," *IEEE Trans. Commun.*, early access, Oct. 2020, doi:10.1109/TCOMM.2020.3033006.
- [15] S. Li, B. Duo, X. Yuan, Y.-C. Liang, and M. Di Renzo, "Reconfigurable intelligent surface assisted UAV communication: Joint trajectory design and passive beamforming," *IEEE Wireless Commun. Lett.*, vol. 9, no. 5, pp. 716-720, May 2020.
- [16] Q. Wu and R. Zhang, "Intelligent reflecting surface enhanced wireless network via joint active and passive beamforming," *IEEE Trans. Wireless Commun.*, vol. 18, no. 11, pp. 5394-5409, Nov. 2019.
- [17] C. Huang, A. Zappone, G. C. Alexandropoulos, M. Debbah, and C. Yuen, "Reconfigurable intelligent surfaces for energy efficiency in wireless communication," *IEEE Trans. Wireless Commun.*, vol. 18, no. 8, pp. 4157-4170, Aug. 2019.
- [18] H. Guo, Y.-C. Liang, J. Chen, and E. G. Larsson, "Weighted sum-rate maximization for reconfigurable intelligent surface aided wireless networks," *IEEE Trans. Wireless Commun.*, vol. 19, no. 5, pp. 3064-3076, May. 2020.
- [19] C. Pan, H. Ren, K. Wang, W. Xu, M. ElKashlan, A. Nallanathan, and L. Hanzo, "Multicell MIMO communications relying on intelligent reflecting surface," *IEEE Trans. Wireless Commun.*, vol. 19, no. 8, pp. 5218-5233, Aug. 2020.
- [20] C. Pan, H. Ren, K. Wang, M. ElKashlan, A. Nallanathan, J. Wang and L. Hanzo, "Intelligent reflecting surface aided MIMO broadcasting for simultaneous wireless information and power transfer," *IEEE J. Sel. Areas Commun.*, vol. 38, no. 8, pp. 1719-1734, Aug. 2020.
- [21] Y. Cao, T. Lv, Z. Lin, W. Ni, and N. C. Beaulieu, "Delay-constrained joint power control, user detection and passive beamforming in intelligent reflecting surface assisted uplink mmWave system," 2019. [Online]. Available: <https://arxiv.org/abs/1912.10030>.
- [22] C. Huang, R. Mo, and C. Yuen, "Reconfigurable intelligent surface assisted multiuser MISO systems exploiting deep reinforcement learning," *IEEE J. Sel. Areas Commun.*, vol. 38, no. 8, pp. 1839-1850, Aug. 2020.
- [23] B. Lyu, D. T. Hoang, S. Gong, and Z. Yang, "Intelligent reflecting surface assisted wireless powered communication networks" in *Proc. IEEE WCNC Workshops*, Seoul, South Korea, Apr. 2020.
- [24] L. Subrt and P. Pechac, "Intelligent walls as autonomous parts of smart indoor environment," *IET commun.*, vol. 6, no. 8, pp. 1004-1010, May, 2012.
- [25] D. Mishra and H. Johansson, "Channel estimation and low-complexity beamforming design for passive intelligent surface assisted MISO wireless energy transfer," in *Proc. IEEE Int. Conf. Acoust., Speech, Signal Process. (ICASSP)*, Brighton, UK, May. 2019, pp. 4659-4663.
- [26] J. Chen, Y. Liang, H. Cheng, and W. Yu, "Channel estimation for reconfigurable intelligent surface aided multi-user MIMO systems," 2019. [Online]. Available: <https://arxiv.org/abs/1912.03619>.
- [27] J. M. Kang, I. M. Kim, and D. I. Kim, "Joint Tx power allocation and Rx power splitting for SWIPT system with multiple nonlinear energy harvesting circuit," *IEEE Wireless Commun. Lett.*, vol. 8, no. 1, pp. 53-56, Feb. 2019.
- [28] G. Ma, J. Xu, Y. Zeng, and M. Moghadam, "A generic receiver architecture for MIMO wireless power transfer with non-linear energy harvesting," *IEEE Signal Proc. Lett.*, vol. 26, no. 2, pp. 312-316, Feb. 2019.
- [29] M. Hong, M. Razaviyayn, Z.-Q. Luo, and J.-S. Pang, "A unified algorithmic framework for block-structured optimization involving big data: With applications in machine learning and signal processing," *IEEE Signal Process. Mag.*, vol. 33, no. 1, pp. 57-77, Jan. 2016.
- [30] Q. Shi, M. Razaviyayn, Z.-Q. Luo, and C. He, "An iteratively weighted MMSE approach to distributed sum-utility maximization for a MIMO interfering broadcast channel," *IEEE Trans. Sig. Process.*, vol. 59, no. 9, pp. 4331-4340, Sep. 2011.
- [31] S. Boyd and L. Vandenberghe. *Convex Optimization*, Cambridge University Press. 2004.
- [32] Z.-Q. Luo, W.-K. Ma, A. M.-C. So, Y. Ye, and S. Zhang, "Semidefinite relaxation of quadratic optimization problems," *IEEE Signal Process. Mag.*, vol. 27, no. 3, pp. 20-34, May 2010.
- [33] T. Scherrer, S. Y. Kim, and C. Yi, "Low complexity, real-time adjusted power management policy using golden section search," in *Proc. Int. SoC Des. Conf. (ISOC)*, Busan, South Korea, Nov. 2013, pp. 229-232.
- [34] Z. Hou, R. Chi, and H. Gao, "An overview of dynamic-linearization-based data-driven control and applications," *IEEE Trans. Ind. Electron.*, vol. 64, no. 5, pp. 4076-4090, May 2017.
- [35] I. M. Johnstone and A. Y. Lu, "Sparse principal components analysis," 2009. [Online]. Available: <https://arxiv.org/abs/0901.4392>.
- [36] Z.-Q. Luo, W.K. Ma, A. M. C. So, Y. Ye, and S. Zhang, "Semidefinite relaxation of quadratic optimization problems," *IEEE Signal Process. Mag.*, vol. 27, no. 3, pp. 20-34, May 2010.
- [37] B. Li, W. Wang, Q. Yin, R. Yang, Y. Li, and C. Wang, "A new cooperative transmission metric in wireless sensor networks to minimize energy consumption per unit transmit distance," *IEEE Commun. Lett.*, vol. 16, no. 5, pp. 626-629, Dec. 2014.